

## Accepted Manuscript

Title: Design and photocatalytic ability of ordered mesoporous TiO<sub>2</sub> thin films

Author: A. Zarubica M. Vasić M.D. Antonijevic M. Randelović M. Momčilović J. Krstić J. Nedeljković



PII: S0025-5408(14)00142-1  
DOI: <http://dx.doi.org/doi:10.1016/j.materresbull.2014.03.015>  
Reference: MRB 7347

To appear in: *MRB*

Received date: 18-3-2014  
Revised date: 18-3-2014  
Accepted date: 18-3-2014

Please cite this article as: A.Zarubica, M.Vasić, M.D.Antonijevic, M.RanDFelović, M.Momčilović, J.Krstić, J.Nedeljković, Design and photocatalytic ability of ordered mesoporous TiO<sub>2</sub> thin films, Materials Research Bulletin <http://dx.doi.org/10.1016/j.materresbull.2014.03.015>

This is a PDF file of an unedited manuscript that has been accepted for publication. As a service to our customers we are providing this early version of the manuscript. The manuscript will undergo copyediting, typesetting, and review of the resulting proof before it is published in its final form. Please note that during the production process errors may be discovered which could affect the content, and all legal disclaimers that apply to the journal pertain.

## Design and photocatalytic ability of ordered mesoporous TiO<sub>2</sub> thin films

A. Zarubica<sup>\*1</sup>, M. Vasić<sup>1</sup>, M. D. Antonijević<sup>2</sup>, M. Ranđelović<sup>1</sup>, M. Momčilović<sup>3</sup>, J. Krstić<sup>4</sup>, J. Nedeljković<sup>3</sup>

<sup>1</sup>Department of Chemistry, Faculty of Science and Mathematics, University of Niš, Višegradska 33, 18000 Niš, Serbia

<sup>2</sup>School of Science, Faculty of Engineering and Science, University of Greenwich, Medway Campus, Chatham Maritime, ME4 4TB, Kent, UK

<sup>3</sup>Vinča Institute of Nuclear Sciences, Belgrade University, P.O. Box 522, 11001 Belgrade, Serbia

<sup>4</sup>University of Belgrade, Institute of Chemistry, Technology and Metallurgy, Department of Catalysis and Chemical Engineering, Belgrade, Serbia

\*Corresponding author: Prof. Dr A. Zarubica, e-mail: azarubicapetrovic@gmail.com; phone: +381 64 41 72 725

### Highlights

- Applicability of new highly ordered mesoporous TiO<sub>2</sub> thin film for photocatalytic degradation of selected organic pollutants was tested.
- Complete degradation of methylene blue (MB) and crystal violet (CV) was achieved.
- Kinetic parameters of photodegradation reactions were correlated to the properties of mesoporous TiO<sub>2</sub> films.
- Dip coating was proved to be effective technique to obtain desired morphology of ordered mesoporous TiO<sub>2</sub> thin films by using polymer templates.

### Abstract

Homogeneous and crack-free TiO<sub>2</sub> films with templated mesoporosity were prepared by **the** dip coating technique using **an** evaporation-induced, self-assembly method. The synthesized mesoporous TiO<sub>2</sub> films were characterized using SEM/TEM, BET and XRD techniques. Degradation reactions of methylene blue and crystal violet dyes were used to test **the** photocatalytic capability of mesoporous TiO<sub>2</sub> films. **The** degradation kinetics of methylene blue

and crystal violet **were investigated over a broad range of initial concentrations of the** organic dyes. The kinetic data were correlated with **the** specific surface area and thickness of mesoporous TiO<sub>2</sub> films, as well as number of reaction cycles.

KEYWORDS: A. nanostructures, A. thin films, B. sol-gel chemistry, C. transmission electron microscopy, D. catalytic properties

## 1. Introduction

**Water pollution is currently a major problem of global significance.** Recalcitrant organic dyes are widely used in **the** textile and photographic industries and present worldwide environmental problems. It is projected that from 1 to 20% of dyestuffs, used in dyeing processes, are released in wastewaters [1,2]. **Even** small concentrations of textile dyes considerably influence the water environment [3]. They can have carcinogenic and mutagenic effects, thus **they are** harmful pollutants for **both** humans and **aquatic** organisms.

Traditional wastewater treatments are not particularly effective for colored effluents. During the past two decades, researchers have been **assessing** unconventional, cost-effective and promising solutions for the complete decolorisation of dye-based contaminants in **the** natural environment. In this context, heterogeneous photocatalysis is considered to be one of the most promising technologies for treatment of water contaminated with toxic organic substances.

Due to their favorable properties TiO<sub>2</sub> based thin films have found extensive commercial applications in water and air refining processes [4-6], as self-cleaning coatings [7], gas sensors [8], electrochromic devices [9], and as TiO<sub>2</sub>-dye composite materials in manufacturing of photovoltaic cells [10,11]. Most of the **foregoing** applications **have been achieved because of the** porous, nanocrystalline structure and large specific surface area of TiO<sub>2</sub> thin films. Several preparative techniques such as sol-gel [12], chemical vapor deposition [13], electrodeposition [14], electrophoresis [15], and ultrasonic spray pyrolysis [16,17] have been developed in order to obtain TiO<sub>2</sub> films with **the** desired properties. The film morphology can be controlled by preparation process parameters such as composition of precursor solution, deposition time, withdrawal rate, etc. Mesoporous TiO<sub>2</sub> films can be deposited either by doctor-blade [18], dip

coating [19,20] or spin coating techniques [21,22]. Recently, **the** evaporation-induced self-assembly method [20,23,24] **using** various precursors and templating **polymers have been used** in order to prepare mesoporous TiO<sub>2</sub> films; **it is accepted that the polymer templates have a significant influence on the porosity of the final material.**

**In** the present study **the** photocatalytic activity of homogeneous and crack-free TiO<sub>2</sub> films with templated mesoporosity, prepared by using **two different** polymers as mesopore directing/generating agents, was tested. **The** degradation kinetics of methylene blue (MB) and crystal violet (CV) dyes **were** investigated as a function of pore size, film thickness and number of reaction cycles.

## 2. Experimental

### 2.1. Preparation of templated TiO<sub>2</sub> thin films

Silicon wafers of W5 quality (dimensions: 25 x 10 x 1.5 mm) were used as substrates cleaned in acetone and ethanol, and then dried at 35 °C for 30 min, before use.

All chemicals were of the highest purity, **and used** as received. Dip coating solutions were typically prepared by dissolving about 6.0 ml of TiCl<sub>4</sub> in 50 ml of dry ethanol (98%) under an inert atmosphere in **a** glove box. During this exothermic process followed **the** increase **in** solution temperature, formation of TiO<sub>2</sub> colloid takes place. After 1 hour, when **the** precursor solution cooled-down to ambient temperature, **an** alcohol-water mixture (50 ml of ethanol and about 10 ml of water) containing either Pluronic F127 tri block copolymer (EO<sub>106</sub>PO<sub>70</sub>EO<sub>106</sub>; m.w. = 12600) or PSM02 polymer (PEO-PBD-PEO; molar weight of PBD part is 10000) was added. **The** molar ratio between TiCl<sub>4</sub> and F127 was adjusted **to** **1** : 0.001, while the molar ratio between TiCl<sub>4</sub> and PSM02 was 1 : 0.01. These solutions were stirred at room temperature for 24 hours **and** **the** addition of deionized water molar ratio between selected solution constituents was adjusted **to** TiCl<sub>4</sub> : EtOH : H<sub>2</sub>O = 1 : 30 : 10.

The TiO<sub>2</sub> films were deposited onto silicon substrates by dip coating combined with **the** evaporation-induced self-assembly method. **The** dip coating procedure was performed in a climate chamber at 25 °C with a withdrawal rate of either 60 or 200 mm/min. **The** relative humidity in **the** climate chamber was adjusted **to** **40%**. All deposited films were initially conditioned at 70 °C for 3 hours **using** synthetic air flow (10 cm<sup>3</sup>/min). Then, calcination of the

TiO<sub>2</sub> films **was** carried out at 400 or 450 °C for 30 min, **again using** synthetic air flow. In both thermal procedures a heating rate **of** 1 °C/min **was employed**.

## 2.2. Characterization of templated TiO<sub>2</sub> thin films

**The** surface morphology and microstructure of the calcined TiO<sub>2</sub> films was studied by scanning electron microscopy (SEM, JEOL 7401F operated at acceleration voltage of 5.0 kV). The **use** of ImageJ software enabled **the** determination of pore size distributions by using **a** statistical approach based on **the** diameter measurement of at least 100 pores **diameters**.

The specific surface area of TiO<sub>2</sub> films was evaluated by using **a** low temperature adsorption/desorption BET method (Micromeritics ASAP 2010 instrument) in N<sub>2</sub> physisorption experiments. **The** specific surface area is expressed as BET m<sup>2</sup> of TiO<sub>2</sub> film per m<sup>2</sup> of substrate planar dimensions.

X-ray diffraction (XRD) measurements were performed using **a** Philips PW-1710 diffractometer with Cu-anticathode and a monochromator **set** at 40 kV and 55 mA. Scherrer's equation was used in order to calculate **the** average crystallite size.

## 2.3. Photocatalytic degradation of organic dyes

Photocatalytic ability of mesoporous TiO<sub>2</sub> thin films was studied using organic dyes, methylene blue (MB) and crystal violet (CV), as model systems. The photochemical reactor consisted of **a** UV lamp (Roth Co., 16W, 2.5 mW/cm<sup>2</sup>,  $\lambda_{\text{max}} = 366$  nm) positioned annular to the 50 ml quartz flask. The rates of photocatalytic degradation of both organic dyes, MB and CV, were followed for different initial concentrations in the **0.005 to 0.03 mM range**. The blank experiments, direct photolysis of MB and CV, were also performed and used as a correction factor. In order to test **the** performance of **the** mesoporous TiO<sub>2</sub> films under long run working conditions, **the** photocatalytic degradation of organic dyes was studied in repeated cycles. The acidity of solutions was not adjusted and pH values were in the range **of** 6.7 to 7.0.

Initial concentrations of organic dyes, as well as their decrease during photodegradation reactions were determined using **a** UV/Vis spectrophotometer (Perkin Elmer Lambda 25).

## 3. Results and Discussion

Typical SEM images of the calcined TiO<sub>2</sub> films deposited onto silicon substrates, obtained by using two different template polymers and two different substrate withdrawal rates, are shown in Figure 1. **The top view of the TiO<sub>2</sub> film prepared by using Pluronic F127 polymer as template (Figure 1a) indicated a complete crack-free surface coverage of substrate. The extensive porosity of the TiO<sub>2</sub> film is noticeable, characterized by a narrow pore size distribution, with an average pore size of about 8 nm. Image of the cross-section of mesoporous TiO<sub>2</sub> film (Figure 1c) revealed a short range, cubic-like ordering of the interconnected pore structure.**

On the other hand, **the dip coating process using PSM02 polymer, as a template, leads to the formation of crack-free mesoporous TiO<sub>2</sub> films with larger pores (20 - 22 nm) compared to Pluronic F127 polymer (Figure 1b). It is obvious that the use of the polymer with the larger molecular mass and consequently larger volume results in the formation of films with larger pore sizes. Image of the cross-section (Figure 1d) of the mesoporous TiO<sub>2</sub> film indicated the elliptical shape of pores and a lower level of their interconnectivity, which can reduce diffusion of reactants through the film during catalytic reactions.**

Cross-section imaging of mesoporous TiO<sub>2</sub> films provided **opportunities** to determine the film thickness as a function of **the dip coating withdrawal rate (Figures 1c and 1d). Based on a limited number of experiments, linear proportionality between film thickness and withdrawal rate was found. For example, a three times thicker TiO<sub>2</sub> film was obtained when the dip coating withdrawal rate was somewhat over three times larger (compare TiO<sub>2</sub> films shown in Figures 1c and 1d). This effect is a consequence of the larger viscous force when the substrate is pulling up the precursor sol at a larger dip coating withdrawal rate. Because of the foregoing, a thicker layer of liquid precursor is deposited over the substrate surface. These results are in agreement with literature data concerning the importance of the substrate withdrawal rate and sol viscosity for the preparation of uniform TiO<sub>2</sub> films using the dip coating technique and titanium alkoxide as a precursor [25].**

Corresponding BET surface areas of mesoporous TiO<sub>2</sub> films obtained by **the dip coating technique in the presence of F127 and PSM02 templates after calcination at 400 °C were found to be 95.7 and 23.4 m<sup>2</sup>/m<sup>2</sup>, respectively. These results are in agreement with the estimated pore size obtained by using a statistical software ImageJ. The average pore size is determined by using the Barrett-Joyner-Halenda (BJH) method [26].** On the other hand, calcination at 450

°C led to a decrease in surface area (47.3 and 19.2 m<sup>2</sup>/m<sup>2</sup> for samples prepared in the presence of F127 and PSM02, respectively). **The decrease in specific surface area is a consequence of extensive particle sintering during the calcination process performed at higher temperature.** Similar BET surface areas of TiO<sub>2</sub> films, obtained by dip coating, **have been reported in the literature [27-30]**, while differences in reported values can be explained in terms of **the different preparation history (substrate type and its roughness, TiO<sub>2</sub> precursor, composition of coating solution and template used in (conventional) the evaporation-induced self-assembly method).**

The crystalline phase composition of the calcined TiO<sub>2</sub> films was analyzed by XRD. The XRD pattern of TiO<sub>2</sub> films, with **sufficient thickness to obtain reliable data (270 nm)**, is shown in Figure 2. The XRD analysis revealed the presence of anatase phase (peaks at 25.3, 37.8, 48.05 and 53.9 °) and a small amount of nonstoichiometric Ti<sub>2</sub>O<sub>3</sub> (peaks/shoulders at 33.1 and 34.8 °). The calculated grain size, based on the broadening of the XRD diffraction peaks, using Scherrer's equation, was found to be 12 nm. This result is in agreement with data obtained by other authors [30,31]. Also, it is important to point out that TiO<sub>2</sub> particles whose size is smaller than 20 nm instead of octahedral have square pyramidal surface structure with one double Ti=O bond [32,33]. Under-coordinated surface titanium atoms are basically active sites with **the capability to efficiently adsorb solutes from the surrounding media, thus improving the photocatalytic ability of TiO<sub>2</sub>.**

It is well-known that **the specific surface area has a significant influence on the photocatalytic efficiency of TiO<sub>2</sub> [34,35]**. In order to quantify this effect **the photocatalytic degradation of two different organic dyes (MB and CV) was investigated under the same experimental conditions using mesoporous TiO<sub>2</sub> films of the same thickness, prepared in the presence of two different polymer templates (F127 and PSM02), having distinct specific surface areas (95.7 and 23.4 m<sup>2</sup>/m<sup>2</sup>, respectively).** **The photocatalytic degradation kinetics of MB and CV are shown in Figure 3a and 3b, respectively.** In the case of both organic dyes, faster degradation kinetics was observed when mesoporous TiO<sub>2</sub> films with larger specific surface area **were used as a photocatalyst.** In addition, **the photocatalytic activity of mesoporous TiO<sub>2</sub> films was tested as a function of their thickness.** As expected, thicker films, due to the larger amount of photocatalyst, induced faster photodecomposition of organic dyes (results are not shown).

Photocatalytic degradation of MB and CV over mesoporous TiO<sub>2</sub> films was investigated as a function of initial concentration of organic dyes **in the 0.005 to 0.03 mM range.** The

degradation kinetic curves for different initial concentrations of MB and CV with usage of mesoporous TiO<sub>2</sub> prepared in the presence of F127 polymer (specific surface area = 95.7 m<sup>2</sup>/m<sup>2</sup>) are shown in Figure 4a and 4b, respectively. Complete decolorization of both organic dyes, under illumination no longer than 1 day, was observed only when **the** initial concentration was sufficiently low. The mesoporous TiO<sub>2</sub> films were peeled-off from the substrate after photocatalytic experiments in order to check their **mass**. For all TiO<sub>2</sub> films used in photocatalytic experiments **a mass** of 30±2 mg was found.

**The** photocatalytic degradation of organic dyes **follows** Langmuir-Hinshelwood kinetics [36], which can be described by **the** following equation:

$$-dC/dt = k_r \cdot K \cdot C_{eq} / (1 + K \cdot C_{eq}) \quad (1)$$

where  $k_r$  is the apparent rate constant,  $K$  is the adsorption coefficient of the substance to be degraded and  $C_{eq}$  is the equilibrium concentration. For very low concentrations of **solutions/pollutants** the Langmuir-Hinshelwood equation simplifies to a pseudo-first-order **kinetic behavior**:

$$-dC/dt = k \cdot C \quad (2)$$

where  $k$  is the pseudo-first-order rate constant.

The pseudo-first-order rate constants determined for different initial concentrations of MB and CV in the photocatalytic degradation reaction using mesoporous TiO<sub>2</sub> films with different specific surface areas (95.7 and 23.4 m<sup>2</sup>/m<sup>2</sup>) but of the same **mass** (30 mg) are collected in Table 1. Based on the **kinetic data for degradation** some general features can be recognized. **Firstly, under the same experimental conditions, the** photocatalytic degradation of CV is slower compared to **the** degradation of MB. **Secondly**, as expected, the degradation of both organic dyes is faster when **the** photocatalyst **exhibits a** larger specific surface area. **Thirdly**, the relative decrease of **the** rate constant with **increase in** initial concentration of both organic dyes is larger for the photocatalyst with **the** smaller specific surface area. This effect can be easily explained **in terms of the greater** occupancy of TiO<sub>2</sub> surface sites with smaller specific surface area by organic dyes. Also, it should be mentioned that in all experiments **the** pH of the solutions was



between 6.7 and 7.0. It is well known that  $\text{TiO}_2$  is amphoteric and that the zero point charge is at  $\text{pH}_{\text{zpc}} \approx 5.9$  [37]. Under **such** experimental conditions, **the** electrostatic attraction between positively charged organic dyes and negatively charged, i.e. deprotonated surface  $-\text{OH}$  groups is **the** driving force for adsorption of organic dyes.

In order to test **the** photocatalytic ability of mesoporous  $\text{TiO}_2$  films under long run working conditions, **the** degradation of both organic **dyes** was **ascertained** in repeated cycles without **the photocatalyst being subject to any cleaning treatments**. The subsequent degradation kinetic curves **for** MB after its complete decolorization are shown in Figure 5. Identical behavior was also observed in the experiments with CV (results are not shown). **It is noticeable** by comparing, for example, the first and the third kinetic cycle **the** photocatalytic ability of  $\text{TiO}_2$  film is not significantly diminished under long run working conditions.

#### 4. Conclusion

**The** dip coating technique with **the use** of templating polymers proved to be a simple way to obtain mesoporous  $\text{TiO}_2$  films with **the** desired properties. Variation of synthetic parameters (composition of precursor solution, withdrawal rate, temperature, etc.) makes **it** possible to control **the** basic characteristics of  $\text{TiO}_2$  films (homogeneity, pore size and their interconnectivity, thickness). The organic dyes (MB and CV), **over a** broad range of initial concentrations, were used as a model system in order to probe **the** photocatalytic capability of synthesized  $\text{TiO}_2$  films. Special attention was paid **to** the influence of pore size and thickness of mesoporous  $\text{TiO}_2$  films, as well as the number of reaction cycles **in terms of** the photocatalytic degradation kinetics of **the** organic dyes. Additional experiments are underway in our laboratories in order to optimize experimental conditions that will improve **the** efficiency of **the** desired photocatalytic reactions.

#### Acknowledgment

This work was financially supported by the Ministry of Education and Science and Technological Development of the Republic of Serbia (research project numbers: ON 172061 and 45020). **The results of this work are parts of the PhD thesis of M. Vasic.**

## References

- [1] D.P. Das, N. Baliarsingh, K.M. Parida, *J. Molec. Catal. A: Chem.* 261 (2007) 254-261.
- [2] C. Galindo, P. Jacques, A. Dalt, *Chemosphere* 45 (2001) 997-1005.
- [3] J.R. Dominguez, J. Beltran, O. Rodriguez, *Catal. Today* 101 (2005) 389-395.
- [4] H. Choi, E. Stathatos, D.D. Dionysiou, *Appl. Catal. B: Environ.* 63 (2006) 60-97.
- [5] L. Andronic, A. Duta, *Mater. Chem. Phys.* 112 (2008) 1078-1082.
- [6] T. Wang, H. Wang, P. Xu, X. Zhao, Y. Liu, S. Chao, *Thin Solid Films* 334 (1998) 103-108.
- [7] I. Sopyan, S. Murasawa, K. Hashimoto, A. Fujishima, *Chem. Lett.* 8 (1994) 723-726.
- [8] V. Demarne, S. Balkanova, A. Grisel, D. Rosenfeld, F. Levy, *Sensor. Actuat. B-Chem.* 14 (1993) 497-498.
- [9] M.P. Cantao, J.I. Cisneros, R.M. Torrese, *J. Phys. Chem.* 98 (1994) 4865-4869.
- [10] Y. Li, J. Hagen, W. Schaffrath, P. Otschik, D. Haarer, *Sol. Energy Mater. Sol. Cells* 56 (1998) 167-174.
- [11] M.G. Kang, N.-G. Park, K.S. Ryu, S.H. Chang, K.-J. Kim, *Sol. Energy Mater. Sol. Cells* 90 (2006) 574-581.
- [12] T. Miki, K. Nishizawa, K. Suzuki, K. Kato, *Mater. Lett.* 58 (2004) 2751-2753.
- [13] A. Conde-Gallardo, N. Castillo, M. Guerrero, *J. Appl. Phys.* 98 (2005) 4-9.
- [14] C. Natarajan, G. Nogami, *J. Electrochim. Acta* 40 (1995) 643-649.
- [15] X. Nie, A. Leyland, A. Matthews, *Surf. Coat. Technol.* 133-134 (2000) 331-337
- [16] M.Dj. Blesic, Z.V. Saponjic, J.M. Nedeljkovic, D.P. Uskokovic, *Mater. Lett.* 54 (2002) 298-302.
- [17] J.M. Nedeljkovic, Z.V. Saponjic, Z. Rakocevic, V. Jokanovic, D.P. Uskokovic, *Nanostruct. Mater.* 9 (1997) 125-128.

- [18] I.M. Arabatzis, T. Stergiopoulos, D. Andreeva, S. Kitova, S.G. Neophytides, P. Falaras, J. Catal. 220 (2003) 127-135.
- [19] J. Yu, X. Zhao, J. Du, W. Chen, J. Sol-Gel Science Techn. 17 (2000) 163-171.
- [20] B. Smarsly, D. Grosso, T. Brezesinski, N. Pinna, C. Boissiere, M. Antonietti, C. Sanchez, Chem. Mater. 16 (2004) 2948-2952.
- [21] H.S. Yun, K. Miyazawa, H.S. Zhou, I. Honma, M. Kuwabara, Adv. Mater. 13 (2001) 1377-1380.
- [22] M.M. Yusuf, H. Imai, H. Hirashima, J. Sol-Gel Sci. Technol. 25 (2002) 65-74.
- [23] J.M. Wu, M. Antonietti, S. Gross, M. Bauer, B.M. Smarsly, Chem. Phys. Chem. 9 (2008) 748-757.
- [24] J. Tang, Y.Y. Wu, E.W. McFarland, G.D. Stucky, Chem. Commun. (2004) 1670-1671.
- [25] E.V. Rebrov, J.C. Schouten, Chem. Eng. Proc. 50 (2011) 1063-1068.
- [26] E.P. Barrett, L.G. Joyner, P.P. Halenda, J. Am. Chem. Soc. 73 (1951) 373-380.
- [27] S. Sokolov, E. Ortel, J. Radnik, R. Kraehnert, Thin Solid Films 518 (2009) 27-35.
- [28] E. Ortel, S. Sokolov, R. Kraehnert, Microporous Mesoporous Mater. 127 (2010) 17-24.
- [29] W. Chen, Y. Geng, X.-D. Sun, Q. Cai, H.-D. Li, D. Weng, Microporous Mesoporous Mater. 111 (2008) 219-227.
- [30] F. Bosc, P. Lacroix-Desmazes, A. Ayral, J. Colloid Inter. Science 304 (2006) 545-548.
- [31] K. Kusakabe, M. Ezaki, A. Sakoguchi, K. Oda, N. Ikeda, Chem. Eng. J. 180 (2012) 245-249.
- [32] L.X. Chen, T. Rajh, W. Jäger, J. Nedeljkovic, M.C. Thurnauer, J. Synchrotron Rad. 6 (1999) 445-447.

- [33] T. Rajh, J.M. Nedeljkovic, L.X. Chen, O. Poluektov, M.C. Thurnauer, J. Phys. Chem. B 103 (1999) 3515-3519.
- [34] L. Zhang, Y. Zhu, Y. He, W. Li, H. Sun, Appl. Catal. B – Environ. 40 (2003) 287-292.
- [35] S.C. Kim, M.C. Heo, S.H. Hahn, C.W. Lee, J.H. Joo, J.S. Kim, I.-K. Yoo, E.J. Kim, Mater. Lett. 59 (2005) 2059-2063.
- [36] K. Vasanth Kumar, K. Porkodi, F. Rocha, Catal. Commun. 9 (2008) 82-84.
- [37] M. Kosmulski, Adv Colloid Interface Sci 99 (2002) 255-264.

## Figure Captions

**Figure 1.** SEM images of mesoporous TiO<sub>2</sub> films obtained in the presence of (a) F127, and (b) PSM02 polymer template (top view). Cross-section of mesoporous TiO<sub>2</sub> films obtained at (c) 60 mm/min, and (d) 200 mm/min withdrawal rate of substrate.

**Figure 2.** The XRD pattern of TiO<sub>2</sub> film with thickness of 270 nm on silicon wafer substrate.

**Figure 3.** Degradation kinetic of MB (a) and CV (b) using mesoporous TiO<sub>2</sub> films as a photocatalyst with different specific surface area (95.7 and 23.4 m<sup>2</sup>/m<sup>2</sup>).

**Figure 4.** Degradation kinetic of MB (a) and CV (b) using mesoporous TiO<sub>2</sub> films as a photocatalyst with 95.7 m<sup>2</sup>/m<sup>2</sup> specific surface area as a function of initial concentration of organic dyes.

**Figure 5.** Degradation kinetic of MB using mesoporous TiO<sub>2</sub> film with 95.7 m<sup>2</sup>/m<sup>2</sup> specific surface are as a function of repeated cycles (initial concentration of MB was 0.01 mM).

**Table 1.** The pseudo-first-order rate constant for different initial concentrations of MB and CV in the photocatalytic degradation reactions over mesoporous TiO<sub>2</sub> films obtained using two

different templating polymers

<b>C<sub>0</sub> (mM)</b>	<b>k<sub>MB</sub> (h<sup>-1</sup>)</b>		<b>k<sub>CV</sub> (h<sup>-1</sup>)</b>	
	<b>F127</b>	<b>PSM02</b>	<b>F127</b>	<b>PSM02</b>
0.005	0.154	0.145	0.139	0.122
0.0075	0.112	0.108	0.100	0.086
0.01	0.079	0.072	0.065	0.058
0.03	0.027	0.022	0.017	0.016

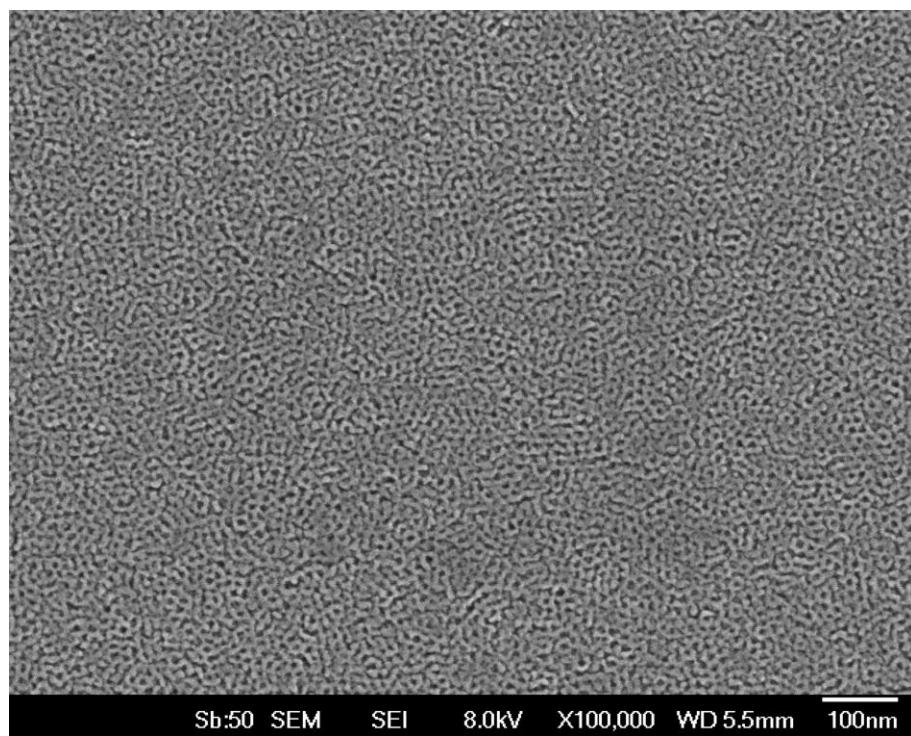


**Fig 1a .**

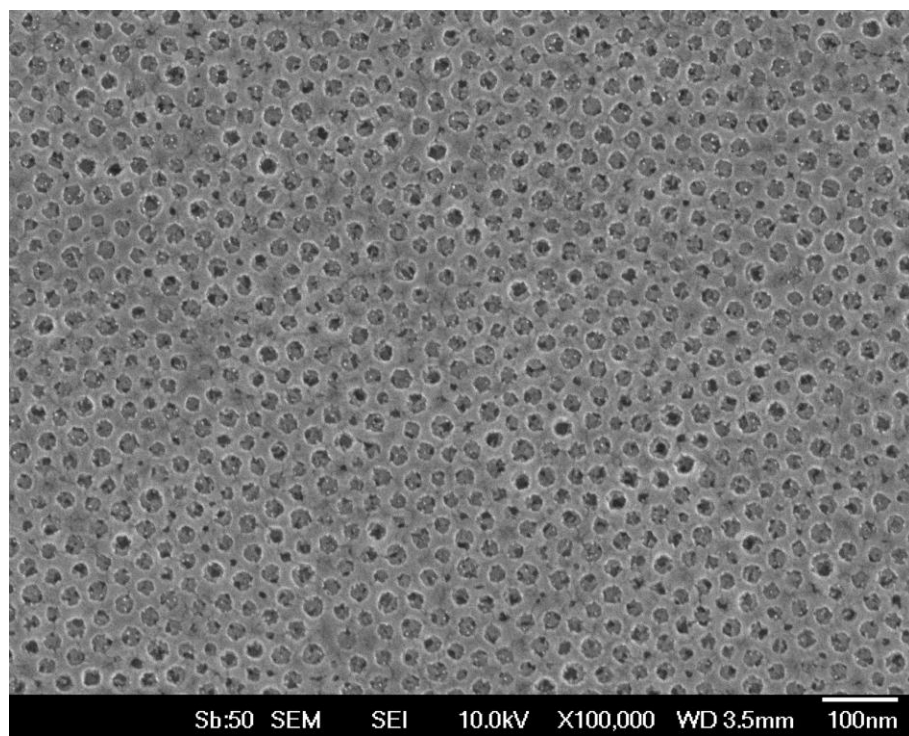


**Fig 1b .**



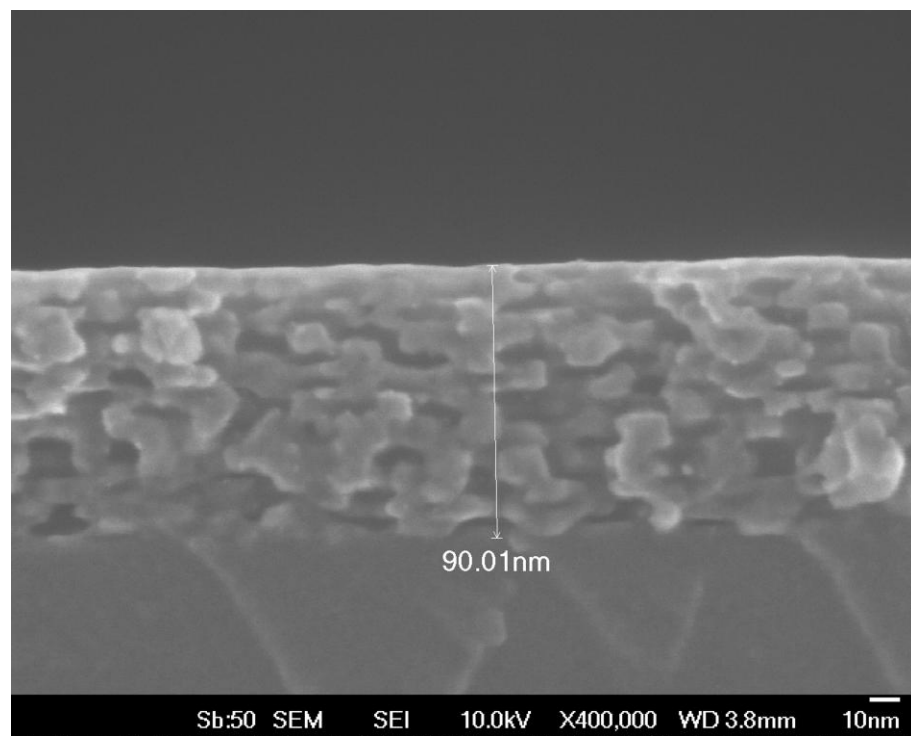


**Fig 1c .**

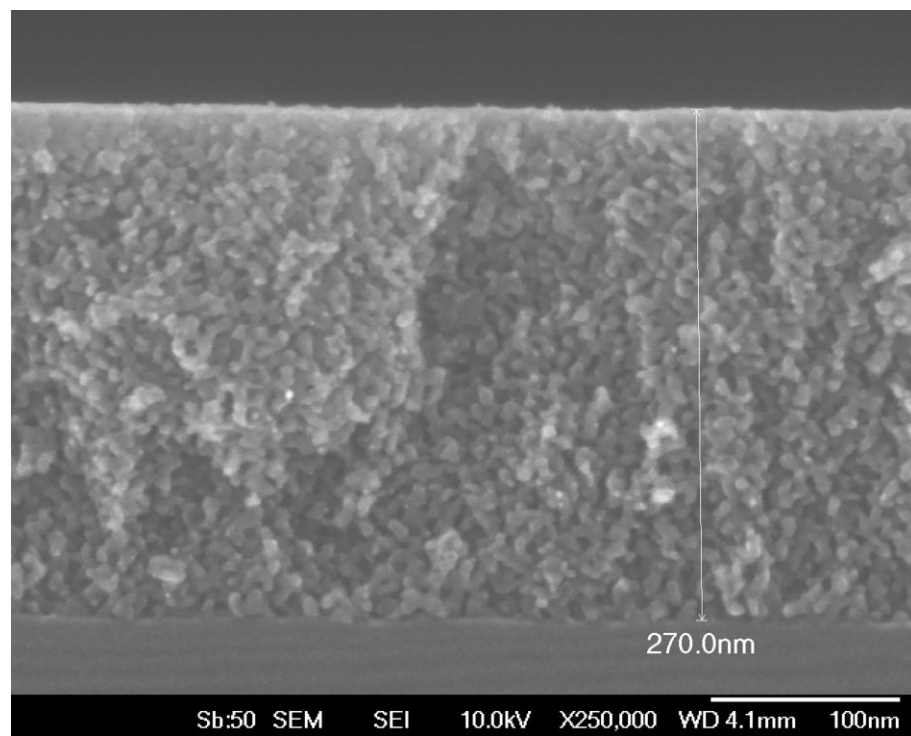


Fig 1d .

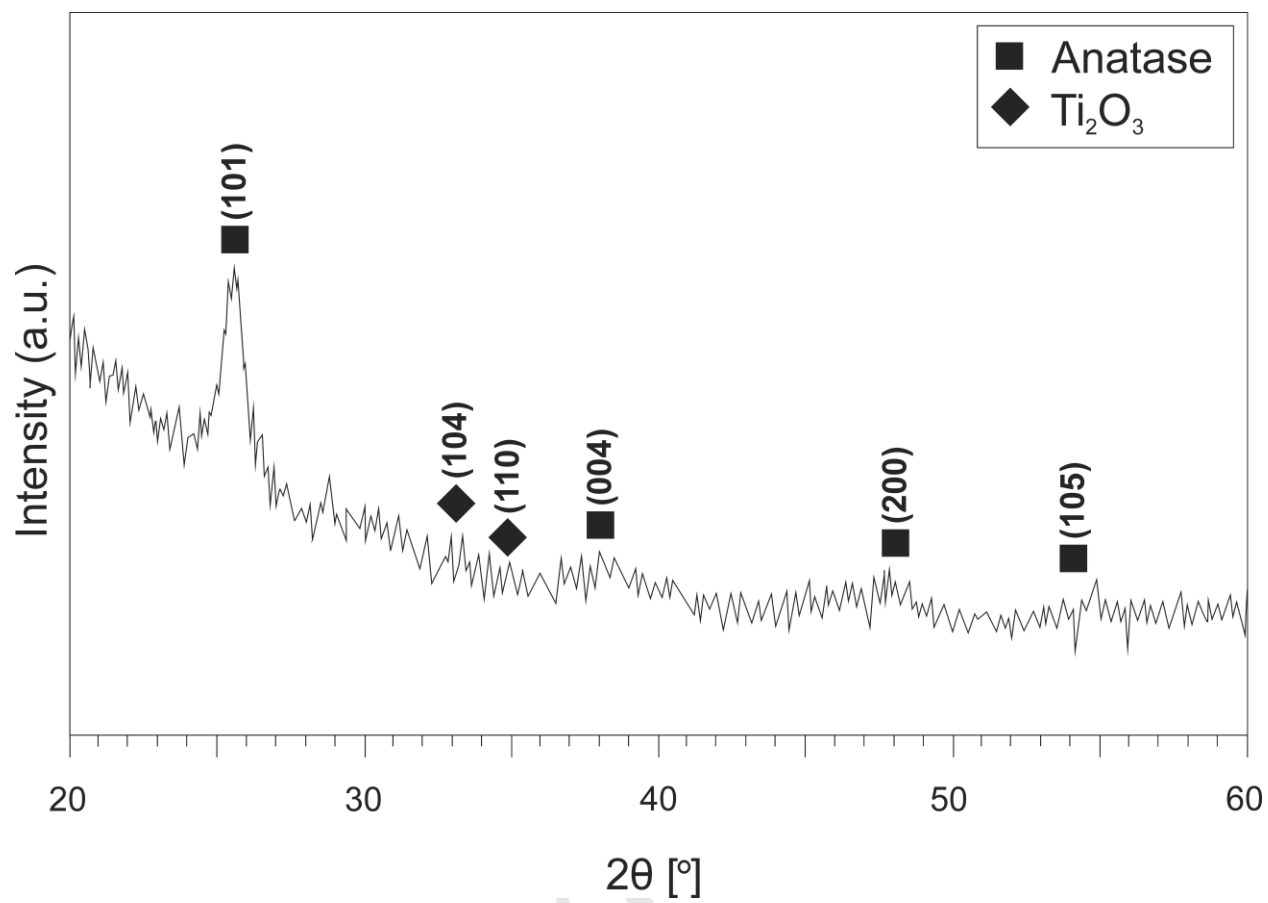


Fig 2 .

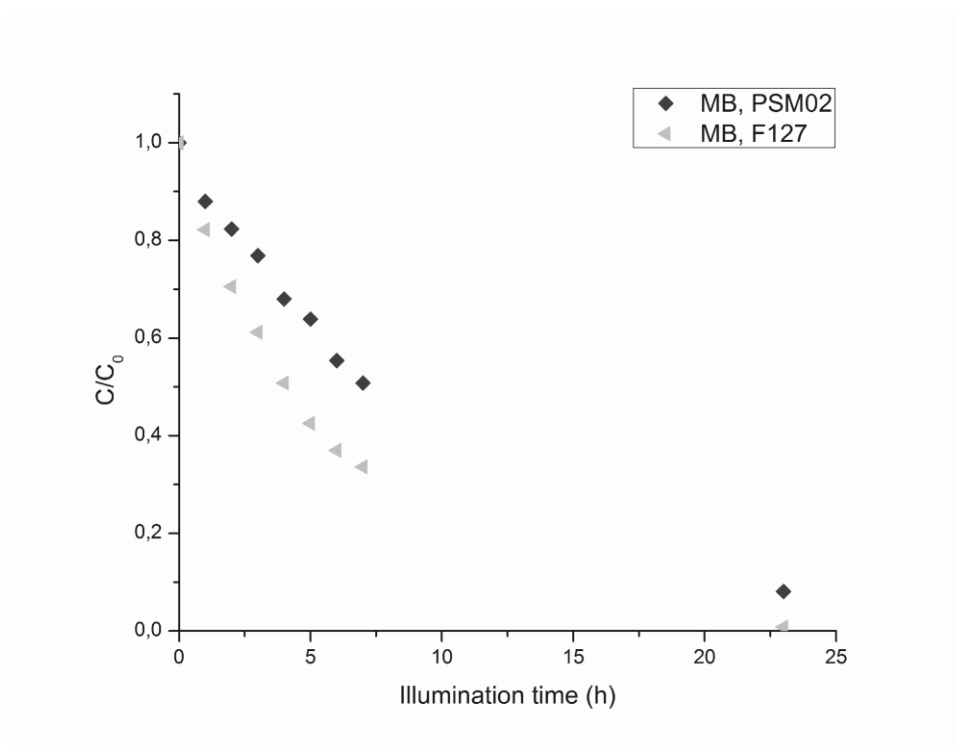


Fig 3a .

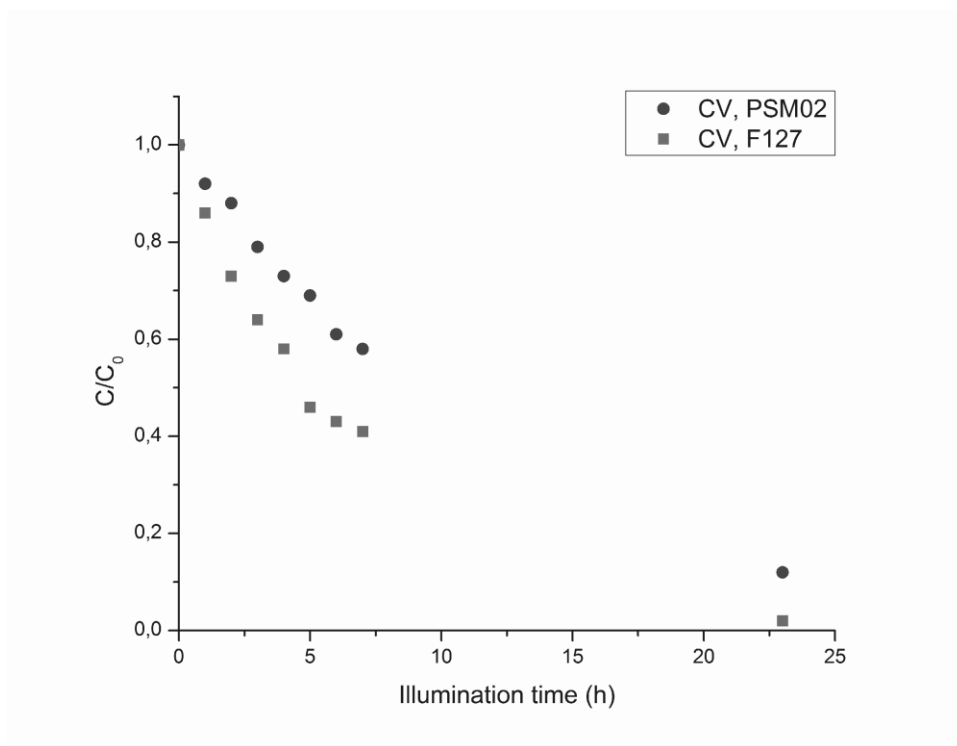
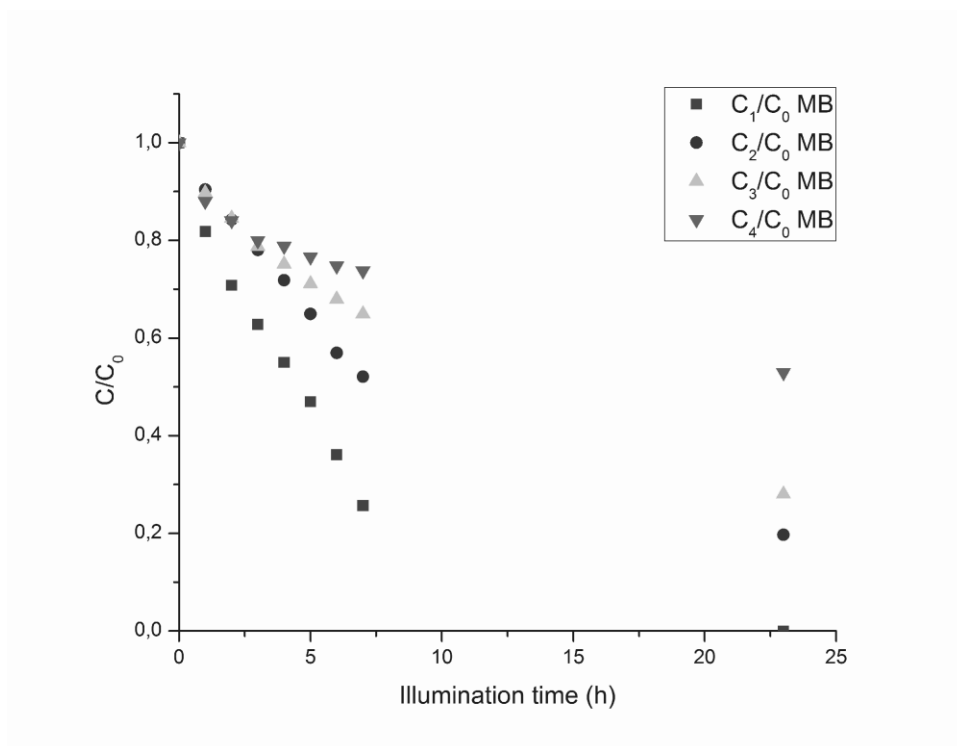
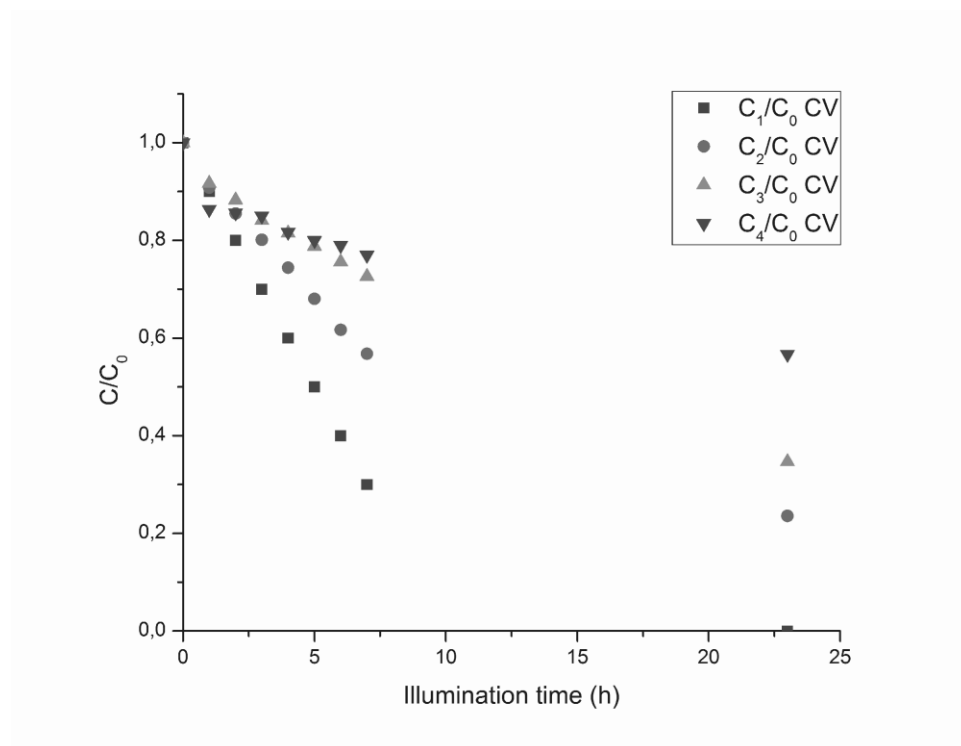


Fig 3b .

**Fig 4a .**

**Fig 4b .**

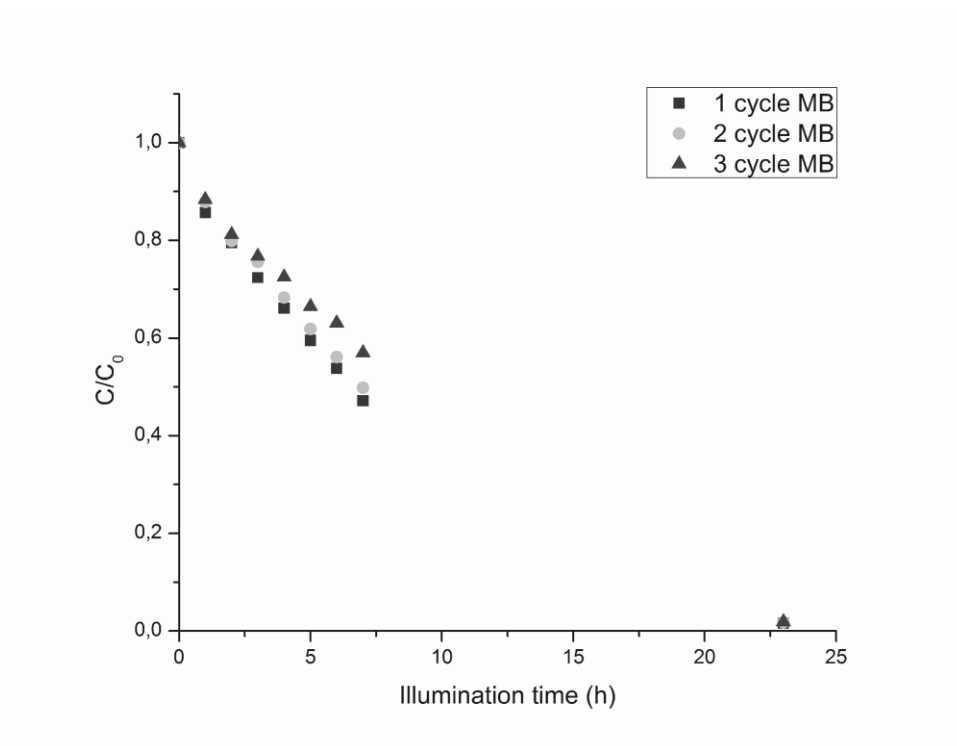


Fig 5 .